**Ninth Canadian Conference on
Earthquake Engineering
Ottawa, Ontario, Canada
26-29 June 2007**

VIRTUAL MASS METHOD FOR EFFECTIVE FORCE TESTING OF STRUCTURES SUBJECT TO DYNAMIC LOADING

C. Chen[1] and J.M. Ricles[2]

ABSTRACT

The Effective Force Test method (EFT) is a relatively new testing technique that has been developed for real-time structural testing. In the EFT method the servo-hydraulic actuator drives the test structure under force control. The EFT method requires that the full structural mass be present in the test structure. This may pose difficulties in the laboratory and raise safety issues. The virtual mass method is proposed in this paper, where only part of the structural mass is required in the test structure to perform an EFT while the rest of the structural mass is modeled analytically. Due to the implicitness of the acceleration response, two different techniques are proposed to update the command force for the actuator. The stability and accuracy of these techniques are analyzed and numerical time history analyses of SDOF structures under ground motion are conducted to validate the virtual mass method. With proper time step sizes, the virtual mass method is shown to have good accuracy when compared with the exact solution.

Introduction

Real-time testing is important to evaluate the performance of innovative systems subjected to dynamic loading, especially for those structures with rate-dependent seismic hazard mitigation devices. Numerous methods have been developed for conducting real-time testing, including shake table testing [Blondet et al. 1988] and the real-time pseudodynamic test method [Nakashima et al. 1992; Darby et al. 1999; Wu et al. 2006] in which the test is performed using a servo-hydraulic actuator under displacement control. Effective force testing (EFT) [Dimig et al. 1999] is a relatively new technique for real-time testing, for which the actuator imposes controlled forces to the test structure.

The excitation forces of a lumped mass structure due to a ground motion depends only on the ground acceleration and the structural mass, and are therefore independent of any structural nonlinearity. If the servo-hydraulic actuator can apply explicit time varying forces accurately onto the test structure, the resulting structural response will be the same as that of the prototype structure subjected to the same earthquake. To conduct EFT testing for lumped mass structures, high-quality servo valves and servo hydraulic controllers are required to enable accurate hydraulic control. As the structure moves under the actuator force, the actuator piston moves with it, which results in changes of the actuator chamber volume and the need for additional oil flow to maintain the force. This phenomenon is particularly severe

[1]Graduate Research Assistant, Dept. of Civil and Environmental Engineering, Lehigh University, Bethlehem, PA 18015
[2] Bruce G. Johnston Professor, Dept. of Civil and Environmental Engineering, Lehigh University, Bethlehem, PA 18015

near the natural frequency of lightly damped structures and results in the inability of the actuator to apply force. It was found by Dyke et al. (1995) and Alleyne et al. (1998) that this inability is attributed to the interaction between the actuator control and the test structure through a “natural velocity feedback” phenomenon. Zhao et al. (2005) developed a natural velocity negation scheme to minimize the effect of the natural velocity feedback, through which the oil flow due to the piston movement is compensated. Experiments (Zhao et al. 2006) on a nonlinear single-degree-of-freedom (SDOF) structure using the EFT method showed that with a natural velocity feedback negation the ability for the actuator to apply force near the natural frequency of the test structure is improved. A comparison of the EFT method results with shaking table test results showed that the EFT method with natural velocity feedback negation is a promising method for real-time testing.

One disadvantage of the EFT method is that the full structural mass must be included in the test setup in order for the proper inertial force to be developed in the test structure. This may pose difficulties in the laboratory and raise safety issues. Chen and Ricles (2006a) proposed a virtual mass method, in which only part of the structural mass is included in the test setup, while the rest of the structural mass is modeled analytically. Due to the implicitness of the acceleration response, two techniques are proposed in this paper for the virtual mass method to update the command forces for the actuators during an EFT with virtual mass. Numerical time history analyses of both linear and nonlinear SDOF structures are conducted to validate the proposed techniques for the virtual mass method. For the purpose of the analysis, the servo-hydraulic system is not considered in this paper.

Formulation of EFT with Virtual Mass for SDOF Structure

For a SDOF structure subject to a ground motion, as shown in Fig. 1(a), the differential equation of motion can be written as

$$m \cdot \ddot{x}(t) + c \cdot \dot{x}(t) + r(t) = -m \cdot \ddot{x}_g(t) = F(t) \tag{1}$$

where m and c are the mass and viscous damping of the SDOF structure, respectively; $\ddot{x}_g$ is the predefined ground acceleration; $\dot{x}$ and $\ddot{x}$ are the velocity and acceleration, respectively; $F(t)$ is the effective force for the SDOF structure subjected to the ground motion; and $r(t)$ is the restoring force of the SDOF structure. For linear elastic structures, the restoring force can be expressed as $r(t) = k \cdot x(t)$, where k is the SDOF linear elastic stiffness and $x(t)$ is the displacement response. It can be observed that the response of the structure subjected to the ground motion is the same as that when the effective force $F(t)$ is applied to the structure. Thus, if the servo-hydraulic actuator can apply the effective force accurately to the test structure, the response is the same for the two test methods.

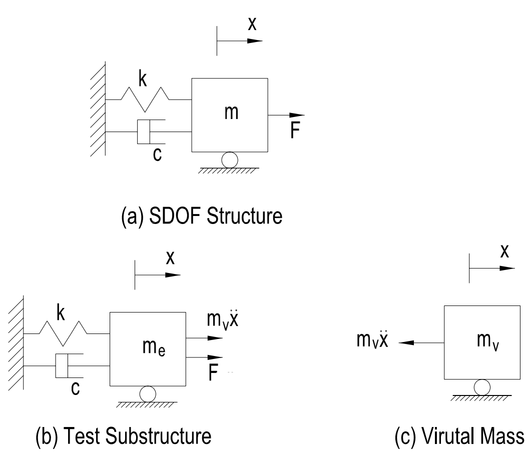

Figure 1. Schematic representation of SDOF structure for an EFT with virtual mass.

To satisfy Eq. 1 for an effective force test, the full structural mass has to be included in the test structure. Chen and Ricles [2006a] proposed a virtual mass method as shown in Fig. 1(b) and 1(c). The equation of motion for the test structure can be written as

$$m_e \cdot \ddot{x}(t) + c \cdot \dot{x}(t) + r(t) = -m \cdot \ddot{x}_g(t) - m_v \cdot \ddot{x}(t) = P(t) \tag{2}$$

where m_e and m_v are the test structure mass and the virtual mass, respectively; and $P(t)$ is the actuator command force applied onto the test structure shown in Fig. 1(b). The sum of m_e and m_v is equal to the total structural mass m. m_v is equal to $\eta \cdot m$ and m_e is equal to $(1-\eta)\cdot m$, where η is referred to as the *virtual mass ratio* in this paper and is a non-negative value between zero and one.

It can be observed from Eq. 2 that when the virtual mass method is used for the EFT method, the structural mass in the test structure is m_e instead of the full structural mass m, and the command force for the actuator is a function of the effective force ($-m \cdot \ddot{x}_g(t)$) and the inertial force of the virtual mass ($-m_v \cdot \ddot{x}(t)$) instead of only the predefined effective force ($-m \cdot \ddot{x}_g(t)$). It can also be observed that the command force $P(t)$ for the actuator in Eq. 2 is implicit for real-time testing, since $P(t)$ is dependent on the implicit structural response of acceleration. Therefore, Eq. 2 has to be solved either by iteration or by using a direct predictor for the acceleration. The temporally discretized form of Eq. 2 can be written as

$$m_e \cdot \ddot{x}_{i+1} + c \cdot \dot{x}_{i+1} + r_{i+1} = -m \cdot \ddot{x}_{g\,i+1} - m_v \cdot \ddot{x}_{i+1} = P_{i+1} \tag{3}$$

where $\dot{x}_{i+1}$ and $\ddot{x}_{i+1}$ are the velocity and acceleration of the SDOF structure at the (i+1)th time step, respectively; $(\ddot{x}_g)_{i+1}$ is the ground acceleration at the (i+1)th time step; and r_{i+1} and P_{i+1} are the restoring force and the actuator command force for the test structure at the (i+1)th time step, respectively.

To update the command force P_{i+1} for the actuator, a direct acceleration predictor is proposed below in Eq. 4, where the previous measured test structure acceleration is utilized as a prediction for the current step acceleration.

$$\tilde{\ddot{x}}_{i+1} = \ddot{x}_i \tag{4}$$

In Eq. (4), $\tilde{\ddot{x}}_{i+1}$ is the predicted acceleration for the (i+1)th step. The acceleration prediction via Eq. (4) is referred to as the *direct acceleration predictor*. With Eq. 4 the command force P_{i+1} for the actuator is made available based on the previous measured acceleration, and the actuator can therefore receive the force command from the controller continuously.

Another method to update the actuator command force is to apply a fixed number of substep iterations to correct the implicit acceleration response, similar to the technique developed by Shing et al. [2002]. This technique is referred to herein as *fixed number of iterations*. In this technique, the time step is divided into a fixed number of smaller substeps. The actuator command force P_{i+1} in Eq. 3 for each substep is updated based on the measured acceleration of the previous substep and the acceleration at the end of the time step is made available by an extrapolation technique using the linear elastic stiffness of the SDOF structure [Chen 2007].

The command force $P_{i+1}^{(k+1)}$ for the actuator at the (k+1)th substep in the (i+1)th time step is calculated as

$$P_{i+1}^{(k+1)} = P_{i+1}^{(k)} + \frac{\tilde{P}_{i+1}^{(k+1)} - P_{i+1}^{(k)}}{n-k} \tag{5}$$

where n is the total number of fixed substeps; and k is a substep index from 0 to (n-1). $\tilde{P}_{i+1}^{(k+1)}$ is the command force predicted at the end of the time step, and is equal to

$$\tilde{P}_{i+1}^{(k+1)} = -m \cdot \ddot{x}_{g\,i+1} - m_v \cdot \ddot{x}_{i+1}^{(k)} \tag{6}$$

In Eq. 6, $\ddot{x}_{i+1}^{(k)}$ is the measured acceleration of the test structure for the kth substep under the actuator force $P_{i+1}^{(k)}$. For the last substep, i.e., $k = n-1$, the acceleration $\ddot{x}_{i+1}^{(n-1)}$ is extrapolated to achieve the acceleration at the end of the (i+1)th time step, where the amount of extrapolated acceleration is:

$$\Delta\ddot{x}_{i+1}^{(k)} = \frac{-e_{i+1}^{(n-1)}}{(m_e + m_v + c\cdot\gamma\cdot\Delta t + k\cdot\beta\cdot\Delta t^2)} \tag{7}$$

In Eq. 7, $e_{i+1}^{(n-1)}$ represents the equilibrium error, where this error for the (n-1)th substep is computed as $e_{i+1}^{(n-1)} = P_{i+1}^{(n-1)} + m\cdot\ddot{x}_{g\,i+1} + m_v\cdot\ddot{x}_{i+1}^{(n-1)}$. Using Eqs. 6 and 7 at the beginning of the next time step, the force command is able to be continuously sent to the actuator without any pauses between time steps.

Stability and Accuracy Analysis of Virtual Mass Method

For the purpose of performing a numerical simulation, an integration algorithm is used to generate the acceleration response of the test structure for an effective force test with virtual mass. When the Newmark family of integration algorithms is used to model the test structure, the variations of displacement and velocity over the time step are defined as [Newmark 1959]

$$\dot{x}_{i+1} = \dot{x}_i + [(1-\gamma)\cdot\Delta t]\cdot\ddot{x}_i + (\gamma\cdot\Delta t)\cdot\ddot{x}_{i+1} \tag{8a}$$

$$x_{i+1} = x_i + (\Delta t)\cdot\dot{x}_i + [(0.5-\beta)\cdot(\Delta t)^2]\cdot\ddot{x}_i + [\beta\cdot(\Delta t)^2]\cdot\ddot{x}_{i+1} \tag{8b}$$

where Δt is the time step size, and β and γ are integration parameters. The discrete transfer function for the Newmark family of integration algorithms can be written in the following general form [Mugan et al. 2001; Chen and Ricles 2006b]

$$G(z) = \frac{X_a(z)}{P(z)} = \frac{n_2\cdot z^2 + n_1\cdot z + n_0}{d_2\cdot z^2 + d_1\cdot z + d_0} \tag{9}$$

where $X_a(z)$ is the discrete z-transform of the acceleration response $\ddot{x}(t)$; and $P(z)$ is the discrete z-transform of external excitation $P(t)$. The coefficients of the discrete transfer function $G(z)$ for the Newmark family of integration algorithms to solve Eq. 3 for a linear elastic SDOF structure are tabulated below in Table 1.

Table 1. Coefficients of $G(z)$ for the Newmark family of integration algorithms.

Numerator		Denominator	
n_2	2	d_2	$2m_e + 2c\cdot\gamma\cdot\Delta t + 2\beta\cdot k\cdot\Delta t^2$
n_1	-4	d_1	$(2\gamma - 4\beta + 1)\cdot k\cdot\Delta t^2 + c\cdot\Delta t\cdot(2-4\gamma) - 4m_e$
n_0	2	d_0	$(2\beta - 2\gamma + 1)\cdot k\cdot\Delta t^2 + c\cdot\Delta t\cdot(2\gamma-2) + 2m_e$

The temporally discretized equation of motion in Eq. 3 can be revised to incorporate the virtual mass with the direct acceleration predictor, whereby

$$m_e\cdot\ddot{x}_{i+1} + c\cdot\dot{x}_{i+1} + r_{i+1} = -m\cdot\ddot{x}_{g\,i+1} - m_v\cdot\ddot{x}_i = P_{i+1} \tag{10}$$

When the direct acceleration predictor is used, a time delay is introduced into the system. The corresponding differential equation of motion for Eq. 10 can be written as

$$m_e \cdot \ddot{x}(t) + c \cdot \dot{x}(t) + r(t) = -m \cdot \ddot{x}_g(t) - m_v \cdot \ddot{x}(t - \Delta t) = P(t) \quad (11)$$

Kyrychko et al. [2006] analyzed a similar problem for real-time dynamic substructuring of a coupled oscillator-pendulum system, and showed that the system in Eq. 11 will become unstable when $m_v > m_e$.

Eq. 10 can be represented schematically by the closed-loop block diagram shown in Fig. 2, where the forward transfer function is the numerically modeled test structure and the feedback loop is the inertial force of the virtual mass using the direct acceleration predictor.

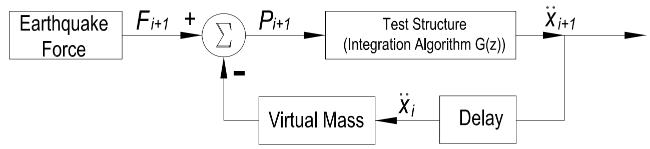

Figure 2. Block diagram of EFT with virtual mass.

The transfer function for the closed loop system in Fig. 2 can be derived using discrete control theory and written in the general form of Eq. 12. The closed loop transfer function reduces to that of the integration algorithm when the virtual mass m_v is equal to zero.

$$G_{cl}(z) = \frac{n_3 \cdot z^3 + n_2 \cdot z^2 + n_1 \cdot z + n_0}{d_3 \cdot z^3 + d_2 \cdot z^2 + d_1 \cdot z + d_0} \quad (12)$$

The stability and accuracy of the closed loop discrete transfer function in Eq. 12 can be determined by its pole locations. It has been shown by Chen and Ricles [2006b] that the poles of the discrete transfer function for an integration algorithm are the same as the eigenvalues of the amplification matrix. If the poles are located within or on the unit circle in the discrete z-domain, the spectral radius is less than one, and the closed loop system is stable. Otherwise, it is unstable [Ogata 1995]. For the discrete transfer function in Eq. 12, two of the poles are complex conjugate poles, which represent the behavior of the structure, while the third pole is a spurious root introduced by the direct acceleration predictor method. The complex conjugate poles can be written as

$$z_{1,2} = \sigma \pm \varepsilon \cdot i = \exp[\overline{\omega} \cdot \Delta t \cdot (-\overline{\xi} \pm i)] \quad (13)$$

where the equivalent damping ratio and the equivalent frequency are defined as $\overline{\xi} = -\ln\left(\sigma^2 + \varepsilon^2\right) / 2\overline{\omega}\Delta t$ and $\overline{\omega} = \tan^{-1}(\varepsilon / \sigma) / \Delta t$, respectively.

To select the proper integration algorithm to model the test structure, the stability and accuracy of the closed loop transfer function in Eq. 12 are investigated. Figs. 3(a) and 3(b) shows the spectral radii for $G_{cl}(z)$ for the cases of $\eta = 0.25$ and $\eta = 0.5$ for an undamped test structure. It can be observed that using Eq. 4, different integration algorithms show different stability limits of $\omega_n \cdot \Delta t$, where ω_n is the SDOF natural frequency. For $\eta = 0.25$, the Newmark explicit method and the Newmark method with linear acceleration show smaller limits of $\omega_n \cdot \Delta t$ than the their original stability limits, while the Newmark method with constant acceleration remains stable for values of $\omega_n \cdot \Delta t$ up to 3.5. For $\eta = 0.5$, Fig. 3(b) shows that only the Newmark method with constant acceleration remains stable. Therefore, the Newmark method with constant acceleration is selected to model the test structure for numerical simulation. It can further be shown that for $\eta > 0.5$ the Newmark method with constant acceleration also will become unstable, which indicates that the virtual mass method with the direct acceleration predictor has a maximum virtual mass ratio of 0.5. This is the same as the delay differential equation analysis result obtained by Kyrychko et al. (2006).

Figs. 3(c) and 3(d) show the equivalent damping and period elongation for the undamped SDOF structure with $\eta = 0.25$. The equivalent damping in Fig. 3(c) due to the direct acceleration predictor for the integration algorithms under consideration is almost the same for values of $\omega_n \cdot \Delta t$ up to 0.4. The period elongation is defined as $PE = (\overline{\omega} - \omega_n)/\omega_n$. It can be observed that the Newmark explicit method shows a period shortening, while the Newmark methods with constant and linear acceleration show a period elongation. For the values of $\omega_n \cdot \Delta t$ less than 0.4, the difference in the period elongation is less than 2% for these integration methods and can be neglected.

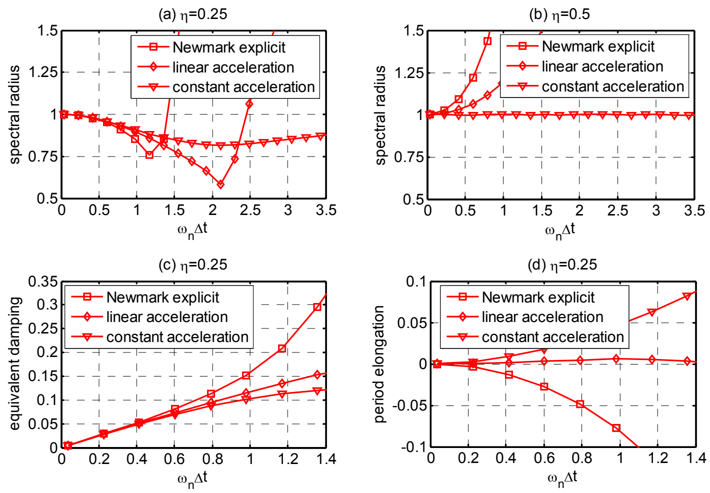

Figure 3. Stability and accuracy of EFT with virtual mass using Direct Acceleration Predictor, undamped structure.

When the technique of a fixed number of substep iterations is used for the EFT method with a virtual mass, it can be proven that for a linear elastic structure, the closed loop transfer function in Eq. 12 reduces to that of the integration algorithm used to model the prototype structure (Chen 2007). When the integration algorithm is unconditional stable, the numerical simulation for the EFT with a virtual mass using the fixed number of iterations method will be unconditional stable, and the accuracy of the numerical simulation will be the same as that of the integration algorithm (Chen 2007).

Numerical Simulation Results

To validate the EFT method with a virtual mass, numerical time history analysis of a SDOF structure subjected to a ground motion are performed. The two proposed techniques for acceleration prediction are used for updating the command force P_{i+1}. Different values of the virtual mass ratio η are considered. The N-S component of 1940 Elcentro earthquake is selected as the ground motion and is scaled to have a peak value of 0.3g.

The linear elastic SDOF structure is assumed to have a structural mass of $m = 5000kg$, a damping ratio of $\xi = 0.02$ and a natural frequency of $\omega_n = 2\pi$. Based on the above assessment, the acceleration of the test structure is simulated with *G(z)* in Fig. 2 using the Newmark method with constant acceleration for the numerical simulation. The time step Δt is 0.002 sec. and 0.02 sec. for the direct and fixed substep prediction methods, respectively. For the purpose of assessing the EFT method with a virtual mass, the numerical simulation results were compared with a solution from the direct integration of Eq. 1 using the

Newmark method with constant acceleration. This converged solution via direct integration is referred to herein as the *exact solution*.

Fig. 4(a) shows the comparison of the displacement time history results for the exact solution to the simulation results of the EFT method with a virtual mass and a direct acceleration prediction with $\eta = 0.25$ and $\eta = 0.50$. It can be observed that the virtual mass method shows good accuracy. A slight undershooting occurs in the displacement response, which can be attributed to the numerical damping introduced by the direct acceleration predictor. With the increase of the virtual mass ratio η, the numerical damping increases and the accuracy of the virtual mass method decreases.

Fig. 4(b) shows the comparison of the displacement time history results for $\eta = 0.75$ and $\eta = 0.95$ when the technique of a fixed number of iterations is used for the acceleration prediction. The number of substeps *n* is 10, whereby the substep size is 0.002 sec. It can be observed that the results are stable and show good accuracy when compared with the exact solution.

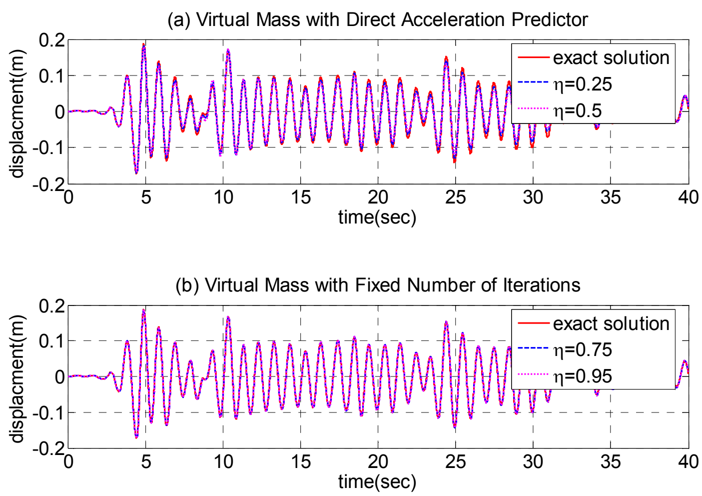

Figure 4. Comparison of EFT with a virtual mass result to exact solution, linear elastic SDOF.

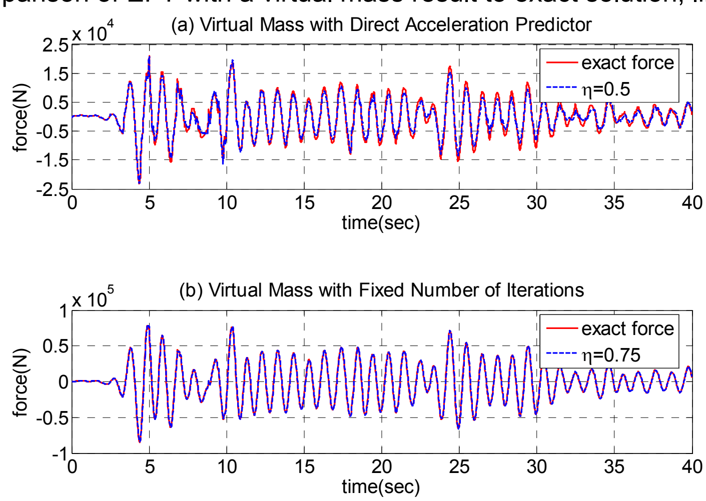

Figure 5. Comparison of command forces of EFT with a virtual mass to exact force, linear elastic SDOF.

When the EFT method with a virtual mass is utilized for the testing of a linear elastic structure, the exact actuator force for the test structure can be calculated based on Eqs. 1 and 3 as

$$\frac{P(s)}{F(s)} = \frac{m_e \cdot s^2 + c \cdot s + k}{m \cdot s^2 + c \cdot s + k} \tag{14}$$

where $P(s)$ is the Laplace transform of the actuator force $P(t)$ applied to the test structure based on the exact solution for linear elastic structural response.

The exact actuator force $P(t)$ for a selected virtual mass ratio based on Eq. 14 is referred to as the *exact force* in the following comparison. Figs. 5(a) and 5(b) show the comparison of the actuator force time history for the virtual mass ratios of $\eta = 0.50$ and $\eta = 0.75$, respectively. It can be observed that the command forces for the actuators are different for the two values of η. It can be determined from Fig. 5, considering that the maximum ground acceleration is 0.3g, that the maximum command force $P(t)$ for the actuator is increased by 50% compared to the maximum excitation force $F(t)$ for $\eta = 0.50$, and 440% for $\eta = 0.75$. When η increases, the second order term of the numerator in Eq. 14 becomes smaller and the resulting actuator command force for the test structure has the high frequency content removed, which helps in the force control of the servo-hydraulic actuator.

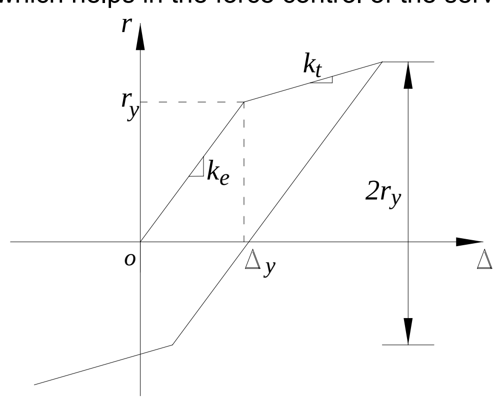

Figure 6. Force-displacement relationship of nonlinear SDOF structure.

A nonlinear SDOF structure is also considered for the time history analysis to validate the virtual mass method. The force-displacement relationship for the SDOF structure is shown in Fig. 6. The nonlinear SDOF structure has the same elastic properties as the linear elastic SDOF structure described previously, with a yield force of $r_y = 1.97kN$ and yield displacement of $\Delta_y = 0.01m$. The post yield stiffness is assumed to be $k_t = 0.2k_e$. The exact solution is calculated by the direct integration of Eq. 1 using the Newmark method with constant acceleration.

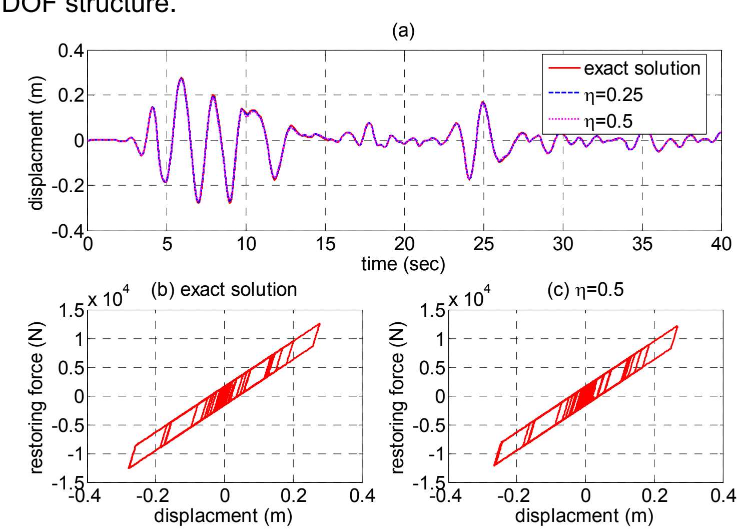

Figure 7. Comparison of EFT with a virtual mass and the Direct Acceleration Predictor result to the exact solution, nonlinear SDOF.

Fig. 7(a) shows the comparison of the exact solution to the numerical results for the EFT method with $\eta = 0.25$ and $\eta = 0.5$ using the direct acceleration predictor. Fig. 7(c) shows the hysteresis of the nonlinear SDOF structure under the actuator command force for the virtual mass ratio of $\eta = 0.5$. Good accuracy can be observed when compared with the exact solution shown in Fig. 7(b).

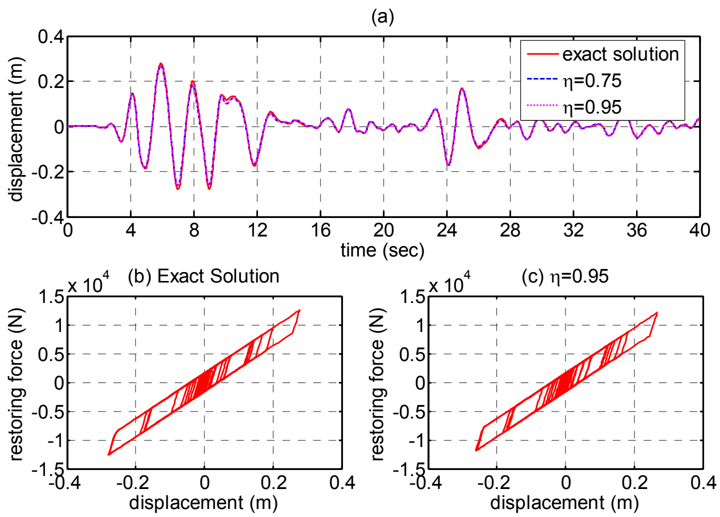

Figure 8. Comparison of EFT with a virtual mass and the Substep Acceleration Predictor result to the exact solution, nonlinear SDOF.

Fig. 8(a) shows the comparison of the exact solution with the numerical results for the EFT method with $\eta = 0.75$ and $\eta = 0.95$ when the technique with a fixed number of iterations is used for updating the actuator command force. Fig. 8(c) shows the hysteresis of the nonlinear SDOF structure under the excitation force with the virtual mass ratio of $\eta = 0.95$. It can be observed that the numerical simulation has good accuracy when compared to the exact solution shown in Fig. 8(b).

Using the two proposed techniques to update the command force for the hydraulic actuator, the structural mass in the test setup is shown to be reduced by 50% for the direct acceleration predictor method based on Eq. 4 and by 95% based on using a fixed number of iterations. The numerical simulation results for the linear and nonlinear SDOF structure show that the virtual mass method is reliable and accurate.

Summary and Conclusions

The EFT method is a promising technique for conducting real-time structural testing to evaluate the performance of innovative structural systems with seismic hazard mitigation devices. To overcome the mass problem in the EFT method, the use of a virtual mass is proposed in this paper, in which only part of the structural mass is required in the test setup and the rest of the structural mass is analytically modeled. To perform an effective force test with a virtual mass in the laboratory, two techniques are proposed to update the command force for the servo-hydraulic actuator. The stability and accuracy of the proposed techniques are investigated for linear elastic structures using the discrete transfer function approach and indicate a virtual mass ratio limit for the acceleration predictor technique based on directly using the acceleration at the end of the prior time step.

With the assumption of perfect hydraulic force control, numerical simulations are performed for both linear and nonlinear SDOF structures subjected to ground motions. The virtual mass method using a direct acceleration predictor shows good accuracy compared with the exact solution when the virtual mass ratio is less than the limit value from the stability analysis. The test structural mass can be reduced by up to 50 percent. A slight difference in the displacement response is observed which is attributed to the numerical damping induced by the acceleration predictor. The technique using a fixed number of iterations to predict the acceleration shows a larger limit for the virtual mass ratio. The numerical simulations for both linear and nonlinear SDOF structures show that the EFT with a fixed number of iterations can reduce the test structural mass by up to 95% and have good accuracy when compared to the exact solution.

Acknowledgments

This paper is based upon work supported by a grant from the Pennsylvania Department of Community and Economic Development through the Pennsylvania Infrastructure Technical Alliance. The support is gratefully appreciated. Any opinions, findings, and conclusions or recommendations expressed in this material are those of the authors and do not necessarily reflect the views of the sponsor.

References

Alleyne, A., Liu, R and Wright, H., 1998. "On the Limitations of Force Tracking Control for Hydraulic Active Suspensions." Proceedings of the American Control Conference, Philadelphia, PA

Blondet, M. and Esparza, C., 1988. "Analysis of shaking table-structure interaction effects during seismic simulation tests." *Earthquake Engineering and Structural Dynamics*, 16, pp. 473-490.

Chen, C. and Ricles, J.M., 2006a. "Effective Force Testing Method using Virtual Mass for Real-Time Earthquake Simulation." Proceedings of the 8th U.S. National Conference on Earthquake Engineering (8NCEE), San Francisco.

Chen, C. and Ricles, J.M., 2006b. "Development of Direct Integration Algorithms for Structural Dynamics Using Discrete Control Theory." *Journal of Engineering Mechanics*, submitted, in review.

Chen, C., 2007. "Development and Numerical Simulation of a Hybrid Effective Force Test Method." *Ph.D. Dissertation*, Lehigh University, Bethlehem, PA.

Darby, A.P., Blakeborough, A. and Williams, M.S., 1999. "Real-Time Substructure Tests using Hydraulic Actuator." *Journal of Engineering Mechanics*, 125, pp. 1133-1139.

Dimig, J., Shield, C., French, C., Bailey, F. and Clark, A., 1999. "Effective Force Testing: A Method of Seismic Simulation for Structural Testing." *Jrnl of Structural Engineering*, 125(9), pp.1028-1037.

Dyke, S.J., Spencer, B.F., Quast, P. and Sain, M.K., 1995. "Role of Control-Structure Interaction in Protective System Design." *Journal of Engineering Mechanics*, 121(2), pp.322-338.

Kyrychko, Y.N., Blyuss, K.B., Buelga, A.G., Hogan, S.J. and Wagg, D.J., 2006. "Real-time Dynamic Substructuring in a Coupled Oscillator-Pendulum System." Proc Royal Society A, 462, pp. 1271-1294.

Mugan, A., Hulbert, G.M., 2001. "Frequency Domain Analysis of Time Integration Methods for Semidiscrete Finite Element Equations, Part II. Hyperbolic and Parabolic-Hyperbolic Problems." International Journal of Numerical Methods in Engineering, 51, pp. 351-376.

Nakashima, M., Kato, H. and Takaoka, E., 1992. "Development of Real-Time Pseudo Dynamic Testing." *Earthquake Engineering and Structural Dynamics*, 21, pp. 79-92.

Newmark, N.M., 1959. "A Method of Computation for Structural Dynamics." *Journal of Engineering Mechanics*, 85, EM3, pp. 67-94.

Ogata, K., 1995. Discrete-Time Control Systems, 2nd Edition, Prentice-Hall, New Jersey.

Shield, C., French, C., Timm, J., 2001. "Development and implementation of the effective force testing method for seismic simulation of large-scale structures." Philosophical Transaction of the Royal Society: Theme Issue on Dynamic Testing of Structures. A 359: 1911-1929.

Shing, P.B., Spacone, E., and Stauffer, E., 2002. “Conceptual Design of a Fast Hybrid Test System at the University of Colorado.” Proceedings of the 7th US National Conference on Earthquake Engineering, Boston, Massachusetts.

Wu, B., Xu, G., Wang, Q., and Williams, M.S., 2006. “Operator-Splitting Method for Real-Time Substructure Testing.” *Earthquake Engineering and Structural Dynamics*, 35, pp. 293-314.

Zhao, J., Shield, C., French, C., and Posbergh, T., 2005. "Nonlinear System Modeling and Velocity Feedback Compensation for EFT." *Journal of Engineering Mechanics*, 131(3), pp.244–253.

Zhao, J., French, C., Shield, C., and Posbergh, T., 2006. "Comparison of Tests of a Nonlinear Structure Using a Shake Table and the EFT Method." *Journal of Structural Engineering*, 132(9), pp.1473-1481.